

The Longitudinal Coupling Impedance  
of an Electron Ring in Cylindrical  
Squirrel Cage Configurations

Peter Merkel

IPP O/39

May 1979



**MAX-PLANCK-INSTITUT FÜR PLASMAPHYSIK**

**8046 GARCHING BEI MÜNCHEN**



**MAX-PLANCK-INSTITUT FÜR PLASMAPHYSIK**  
**GARCHING BEI MÜNCHEN**

The Longitudinal Coupling Impedance  
of an Electron Ring in Cylindrical  
Squirrel Cage Configurations

Peter Merkel

IPP O/39

May 1979

*Die nachstehende Arbeit wurde im Rahmen des Vertrages zwischen dem  
Max-Planck-Institut für Plasmaphysik und der Europäischen Atomgemeinschaft über die  
Zusammenarbeit auf dem Gebiete der Plasmaphysik durchgeführt.*



Abstract

The longitudinal coupling impedance matrix  $Z_{m,n}$  is investigated for a relativistic electron ring in a coaxial configuration consisting of a conducting cylinder and an axially slit cylinder, a so-called "squirrel cage". The calculation is based on the solution of a special Hilbert problem. Computational results showing the dependence of  $Z_{m,n}$  on the geometry, the number and width of the slits and on the mode number  $n$  are presented. For  $n \ll N$  an approximate formula of  $Z_{m,n}$  is given.



## I. Introduction

In order to achieve effective collective acceleration of ions in relativistic electron ring accelerators [1], [2], [3], it is necessary to avoid the negative mass instability [4]. To obtain stable rings with high electron number and small minor ring dimensions, the coupling impedance has to be as small as possible. This can be attained by applying conducting walls, i.e. coaxial cylinders, close to the ring, which keep the coupling impedance sufficiently small [5], [6], [7].

For axial focussing of the rings axially slit conducting cylinders, so-called "squirrel cages", have been successfully used [8], [9], [10]. Concerning the negative mass instability the question therefore arises whether and to what extent the slits of finite width affect the impedance of the ring.

In a previous paper [11] we approximated the squirrel cage by a cylinder of anisotropic conductivity. The advantage of that model was that by preserving the axisymmetry the calculation was straight forward. But the results might be relevant only for perturbation wave lengths large compared with the squirrel cage period. We found a rather drastic increase of the impedance compared with the conducting cylinder case, which was mainly due to the presence of a TEM mode propagating undamped axially along the cylinder.

This effect can be expected to as well be present in the squirrel cage geometry. But in order to get the value of the impedance quantitatively and its dependence on the various parameters such as width and number of strips, one has to consider the real periodic structure, where the electromagnetic field has to satisfy the boundary conditions on the conducting strips and the non-conducting slits.

Beloshitsky and Perelstein [12] have calculated the impedance of an E-layer in a squirrel cage. But the results are not rele-



vant to the ring impedance, particularly because the above-mentioned TEM mode does not occur in the E-layer case. For a plane geometry Zhabitsky [13] published a calculation of the impedance. An electron beam moves parallel to a plane in which conducting strips are periodically arranged perpendicular to the beam. But this calculation is not correct. The solution does not satisfy the boundary conditions on the strips.

In the present paper the coupling impedance of the ring is calculated for a coaxial configuration consisting of the electron ring, a squirrel cage and a conducting cylinder with arbitrary radii (Fig.1). In Section II the derivation of the coupling impedance is given. From the general formula a very useful approximation for  $n/N \ll 1$  ( $n$  = mode number,  $N$  = number of strips) is obtained. In Section III numerically evaluated results are presented. The dependence of the impedance on various parameters such as number and width of slits, radii of squirrel cage and cylinder, and mode number is discussed.

The impedance calculation leads to a problem which is known in the theory of singular integral equations [14] as the Hilbert problem. The solution of the special Hilbert problem, which we have used, is given by Agranovich, Marchenko, Shestopalov [15] and by Marchenko and Sologub [16]. A slightly modified derivation of the solution and some extensions are given in the Appendix.

## II. The Calculation of the Longitudinal Coupling Impedance

The force driving the negative mass instability [4] is the azimuthal electric field which is produced by the perturbation of the ring charge and current. Assuming an electron ring with radius  $R$  infinitely thin in the radial direction and with an axial length  $2a$ , the ring current perturbation proportional to  $e^{-i\omega t}$  can be written as the Fourier sum

$$(8) \quad b_n(r, r') = \begin{cases} \frac{1}{2} \left( \frac{r}{r'} \right)^n & r < r' \\ \frac{1}{2} \left( \frac{r'}{r} \right)^n & r > r' \end{cases} \quad , \quad s = (R - \frac{1}{2}a)^{1/2}$$

$$(3) \quad \Delta \Pi + \omega \Pi = \frac{1}{2} \sum_{n=0}^{\infty} \frac{J_n^2(xr)}{H_n^{(1)}(xr)} \quad , \quad \frac{r}{R} > \frac{r'}{R} \quad , \quad \frac{r}{R} < \frac{r'}{R}$$



$$(1) \quad \underline{j} = \underline{e}_\varphi \sum_{n=-\infty}^{+\infty} I_n \delta(r-R) \left( \frac{\theta(z+a) - \theta(z-a)}{2a} \right) e^{i(n\varphi - \omega t)},$$

where  $(r, \varphi, z)$  are cylindrical coordinates,  $\theta(z)$  is the Heaviside function and  $\underline{e}_\varphi$  is the unit vector in the  $\varphi$ -direction. The perturbation of the charge density follows from the continuity equation  $\dot{\rho} + \text{div } \underline{j} = 0$ .

Because the electric field depends linearly on the current, one can define an impedance matrix  $Z_{m,n}$ , which gives the dependence of the  $m$ -th Fourier component of the  $E_\varphi$ -field on the Fourier components  $I_n$  of the current

$$(2) \quad \frac{1}{2a} \int_{-a}^a E_{\varphi,m}(R, z) dz = - \frac{1}{2\pi R} \sum_{n=-\infty}^{+\infty} Z_{m,n} I_n.$$

We took the mean value of the  $E_\varphi$  field averaged over the ring cross-section. In the theory of the negative mass instability to which we refer the influence of the minor ring dimensions on the instability is neglected. Only the mean value of  $E_\varphi$  therefore has a relevant meaning.

The impedance matrix  $Z_{m,n}$  depends on the boundary conditions for the electromagnetic field, which are determined by the geometry of the conductors surrounding the electron ring. In the present paper we consider an electron ring inside or outside a coaxial conducting configuration consisting of a cylinder with radius  $P$  and a squirrel cage with radius  $T$ . The squirrel cage is a structure made of  $N$  equidistant strips of width  $D$  and slits of width  $L-D$  (Fig.1).

To calculate the  $E_\varphi$ -field produced by the time-periodic charge and current given by eq.(1), we use the Hertz potential  $\underline{\Pi}$ . For  $\underline{\Pi} = \underline{\Pi}(r, \varphi, z) e^{-i\omega t}$  the Maxwell equations are (velocity of light  $c = 1$ )

$$(3) \quad \Delta \underline{\Pi} + \omega^2 \underline{\Pi} = -i \frac{4\pi}{\omega} \underline{j}.$$



The electric and magnetic fields are obtained from  $\Pi$  by

$$(4) \quad \begin{aligned} \underline{B} &= -i\omega \cdot \text{curl } \Pi, \\ \underline{E} &= \text{grad div } \Pi + \omega^2 \Pi. \end{aligned}$$

To get the retarded solution, one has to add a small positive imaginary part  $i\epsilon$  ( $\epsilon > 0$ ) to the real positive  $\omega$ .

For the geometry to be considered it is appropriate to start with Fourier transformations with respect to  $z$  and  $\varphi$ :

$$(5) \quad \Pi = \sum_{n=-\infty}^{+\infty} \int_{-\infty}^{+\infty} dk \begin{pmatrix} \Pi_{r,n}(k,r) \\ \Pi_{\varphi,n}(k,r) \\ \Pi_{z,n}(k,r) \end{pmatrix} e^{i(kz+n\varphi-\omega t)}$$

The general solution for  $\Pi$  produced by an arbitrary charge and current distribution on the surface of a cylinder with radius  $r'$ , where the charge and the current satisfy the continuity equation, is given by

$$(6) \quad \begin{aligned} \Pi_{r,n}(k,r) &= -A_n(k) \frac{\pi r'}{\omega} a_n^+(r,r'), \\ \Pi_{\varphi,n}(k,r) &= A_n(k) \frac{i\pi r'}{\omega} a_n^-(r,r'), \\ \Pi_{z,n}(k,r) &= C_n(k) \frac{\pi}{\omega} b_n(r,r'), \end{aligned}$$

where  $A_n$ ,  $C_n$  are arbitrary coefficients and

$$(7) \quad a_n^{\pm}(r,r') = \frac{1}{2} (b_{n-1}(r,r') \pm b_{n+1}(r,r'))$$

with

$$(8) \quad b_n(r,r') = \begin{cases} J_n(sr) H_n^{(1)}(sr'), & r \leq r' \\ J_n(sr') H_n^{(1)}(sr), & r > r' \end{cases}, \quad s = (\omega^2 - k^2)^{1/2}$$

For later use we define, in addition,

$$(9) \quad b'_n(r, r') = \begin{cases} J'_n(sr) H_n^{(1)'}(sr') rr' s^2, & r \leq r', \\ J'_n(sr') H_n^{(1)'}(sr) rr' s^2, & r > r'. \end{cases}$$

The  $J_n$ ,  $J'_n$ ,  $H_n^{(1)}$ ,  $H_n^{(1)'}$  are the Bessel function and the Hankel function of the first kind and their derivatives.

The potential of the ring current given by eq.(1) is a special solution of eq.(6) with coefficients

$$(10) \quad A_n^{\text{ring}}(k) = I_n \frac{\sin ka}{ka}, \quad C_n^{\text{ring}}(k) = 0.$$

The field of the configuration consisting of the ring, the cylinder and the squirrel cage is the sum of the fields produced by the ring current and charge and by the image currents and charges induced in the cylinder and the squirrel cage. Given the ring current the image currents in the cylinder and the squirrel cage are determined by the requirement that the electric field is normal on the conductors.

For the Hertz potential produced by the current in the squirrel cage one starts with the ansatz

$$(11) \quad \underline{\Pi}^{\text{sq}} = \frac{\pi}{\omega} \sum_{\ell=-\infty}^{+\infty} \int_{-\infty}^{+\infty} dk \begin{pmatrix} -A_{\ell}^{\text{sq}T} a_{N\ell+n}^{+}(r, T) \\ iA_{\ell}^{\text{sq}T} a_{N\ell+n}^{-}(r, T) \\ C_{\ell}^{\text{sq}} b_{N\ell+n}(r, T) \end{pmatrix} e^{i(N\ell+n)\varphi} e^{i(kz-\omega t)}$$

and for the potential  $\underline{\Pi}^{\text{cyl}}$  produced by the current in the cylinder with a corresponding ansatz replacing the radius  $T$  by  $P$  and the coefficients  $A_{\ell}^{\text{sq}}$ ,  $C_{\ell}^{\text{sq}}$  by  $A_{\ell}^{\text{cyl}}$ ,  $C_{\ell}^{\text{cyl}}$ . We have made use of the symmetry of the problem, from which it follows that the only non-vanishing Fourier components are  $m = N\ell+n$ ,  $\ell = 0, \pm 1, \pm 2, \dots$ .



The unknown coefficients  $A_\ell^{sq}$ ,  $C_\ell^{sq}$ ,  $A_\ell^{cyl}$ ,  $C_\ell^{cyl}$  are determined by the requirements that  $E_z = E_\varphi = 0$  on the cylinder and on the strips of the squirrel cage, and that the electromagnetic field is continuous in the slits of the squirrel cage.

The conditions  $E_z = E_\varphi = 0$  on the cylinder lead to the following equations for the coefficients:

$$(12) \quad b_{N\ell+n}(P,T)D_\ell^{sq} + b_{N\ell+n}(P,P)D_\ell^{cyl} + b_n(R,P) \frac{\sin ka}{ka} \delta_{\ell 0} I_n = 0,$$

$$\ell = 0, \pm 1, \pm 2, \dots$$

and

$$(13) \quad b'_{N\ell+n}(P,T)A_\ell^{sq} + b'_{N\ell+n}(P,P)A_\ell^{cyl} + b'_n(R,P) \frac{\sin ka}{ka} \delta_{\ell 0} I_n = 0,$$

$$\ell = 0, \pm 1, \pm 2, \dots$$

where one has introduced the combination of the coefficients

$$(14) \quad D_\ell^{sq} = ((N\ell+n)kA_\ell^{sq} + s^2 C_\ell^{sq}) \frac{1}{nk},$$

$$D_\ell^{cyl} = ((N\ell+n)kA_\ell^{cyl} + s^2 C_\ell^{cyl}) \frac{1}{nk}.$$

The condition  $E_z = E_\varphi = 0$  on the strips of the squirrel cage gives

$$(15) \quad \sum_{\ell=-\infty}^{+\infty} (b'_{N\ell+n}(T,T)A_\ell^{sq} + b'_{N\ell+n}(P,T)A_\ell^{cyl}) e^{iN\ell\varphi} =$$

$$= -b'_n(R,T) \frac{\sin ka}{ka} I_n, \quad \varphi \in \text{strips}$$

and

$$(16) \quad \sum_{\ell=-\infty}^{+\infty} (b_{N\ell+n}(T,T)D_\ell^{sq} + b_{N\ell+n}(P,T)D_\ell^{cyl}) e^{iN\ell\varphi} =$$

$$= -b_n(R,T) \frac{\sin ka}{ka} I_n, \quad \varphi \in \text{strips},$$

and the requirement that the electric and magnetic fields be continuous in the slits leads to the equations

$$(17) \quad \sum_{\ell=-\infty}^{+\infty} A_{\ell}^{sq} e^{iN\ell\varphi} = 0, \quad \varphi \in \text{slits}$$

and

$$(18) \quad \sum_{\ell=-\infty}^{+\infty} D_{\ell}^{sq} e^{iN\ell\varphi} = 0, \quad \varphi \in \text{slits}.$$

Eliminating  $A_{\ell}^{cyl}$ ,  $D_{\ell}^{cyl}$  in eqs.(15) and (16) by using eqs.(12) and (13) one gets

$$(19) \quad \sum_{\ell=-\infty}^{+\infty} \left( b'_{N\ell+n}(T, T) - \frac{b'^2_{N\ell+n}(P, T)}{b'_{N\ell+n}(P, P)} \right) A_{\ell}^{sq} e^{iN\ell\varphi} = \varphi \in \text{strips}$$

$$= - \left( b'_n(R, T) - \frac{b'_n(P, T) b'_n(R, P)}{b'_n(P, P)} \right) \frac{\sin ka}{ka} I_n,$$

and

$$(20) \quad \sum_{\ell=-\infty}^{+\infty} \left( b_{N\ell+n}(T, T) - \frac{b^2_{N\ell+n}(P, T)}{b_{N\ell+n}(P, P)} \right) D_{\ell}^{sq} e^{iN\ell\varphi} = \varphi \in \text{strips}$$

$$= - \left( b_n(R, T) - \frac{b_n(P, T) b_n(R, P)}{b_n(P, P)} \right) \frac{\sin ka}{ka} I_n,$$

To determine  $A_{\ell}^{sq}$  and  $D_{\ell}^{sq}$ , one has to solve the systems of eqs.(17), (19) and eqs.(18), (20). Problems of this type are treated by Agranovich et al. [15] and by Marchenko and Sologub [16].

Because the infinite series do not converge uniformly in  $\varphi$ , approximate solutions for  $A_{\ell}^{sq}$  and  $D_{\ell}^{sq}$  cannot be obtained by truncating the series at some finite order. The method of solving the equations is based on exact solutions of special Hilbert problems for arcs (see Appendix).

From the uniform asymptotic expansion for large-order  $m$  of the Bessel and Hankel functions [17], the asymptotic expansions for  $b_m(r, r')$  and  $b'_m(r, r')$  are found to be

$$(21) \quad b_m(r, r') = - \frac{i}{\pi |m|} \begin{cases} \left(\frac{r}{r'}\right)^{|m|}, & r \leq r' \\ \left(\frac{r'}{r}\right)^{|m|}, & r > r' \end{cases} \quad |m| \rightarrow \infty,$$

and

$$(22) \quad b'_m(r, r') = -m^2 b_m(r, r') \quad , \quad |m| \rightarrow \infty.$$

From this it follows that the coefficient of  $A_\ell^{sq}$  in eq.(19) behaves like  $|\ell|$  for large  $\ell$ , and the coefficient of  $D_\ell^{sq}$  in eq.(20) like  $1/|\ell|$  for large  $\ell$ . Now, replacing the coefficients of  $A_\ell^{sq}$  and  $D_\ell^{sq}$  by their asymptotic values, the systems of equations for  $A_\ell^{sq}$  and  $D_\ell^{sq}$  can be solved exactly, as shown in the Appendix.

To get an approximate solution of the real systems, one makes use of this fact by rewriting eqs.(17) to (20) in the following form:

One defines  $m_0$  and  $\mu$  by

$$(23) \quad m_0 + \mu = \frac{n}{N}, \quad m_0 \text{ integer}, \quad 0 \leq \mu < 1$$

and introduces

$$(24) \quad \varepsilon_{\ell+m_0} = 1 + \frac{i\pi}{|N\ell+n|} \left( b'_{N\ell+n}(T, T) - \frac{b'^2_{N\ell+n}(P, T)}{b'_{N\ell+n}(P, P)} \right),$$

$$(25) \quad \eta_{\ell+m_0} = 1 - i\pi |N\ell+n| \left( b_{N\ell+n}(T, T) - \frac{b^2_{N\ell+n}(P, T)}{b_{N\ell+n}(P, P)} \right).$$



Furthermore, one defines

$$(26) \quad Y_{\ell+m_0} = \frac{i k a N}{\pi \sin k a I_n \left( b'_n(R, T) - \frac{b'_n(P, T) b'_n(R, P)}{b'_n(P, P)} \right)} A_{\ell}^{sq},$$

$$(27) \quad x_{\ell+m_0} = - \frac{i k a}{\pi N \sin k a I_n \left( b_n(R, T) - \frac{b_n(P, T) b_n(R, P)}{b_n(P, P)} \right)} D_{\ell}^{sq}.$$

In terms of these new quantities eqs.(17) to (20) then become

$$(28) \quad \sum_{\ell=-\infty}^{+\infty} Y_{\ell} e^{i\ell\varphi} = 0, \quad \varphi_0 < |\varphi| < \pi,$$

$$(29) \quad \sum_{\ell=-\infty}^{+\infty} |\ell+\mu| (1-\varepsilon_{\ell}) Y_{\ell} e^{i\ell\varphi} = e^{im_0\varphi}, \quad \varphi_0 > |\varphi|,$$

and

$$(30) \quad \sum_{\ell=-\infty}^{+\infty} x_{\ell} e^{i\ell\varphi} = 0, \quad \varphi_0 < |\varphi| < \pi,$$

$$(31) \quad \sum_{\ell=-\infty}^{+\infty} \frac{1}{|\ell+\mu|} (1-\eta_{\ell}) x_{\ell} e^{i\ell\varphi} = e^{im_0\varphi}, \quad \varphi_0 > |\varphi|.$$

where one has substituted  $N\varphi \rightarrow \varphi$  and  $\varphi_0$  is defined as  $\varphi_0 = \pi D/L$ . For the  $\varepsilon_{\ell}$ ,  $\eta_{\ell}$  it holds that  $\varepsilon_{\ell} \rightarrow 0$ ,  $\eta_{\ell} \rightarrow 0$  for  $|\ell| \rightarrow \infty$ . Transferring all terms containing  $\varepsilon_{\ell}$  and  $\eta_{\ell}$  to the right side and considering them as known for a moment, eqs.(28) to (31) are Hilbert problems, which are solved in the Appendix.

The solutions are infinite systems of linear equations for the  $Y_{\ell}$  and  $x_{\ell}$ . From eqs.(A32), (A33), (A37) and (A39) one gets

$$(32) \quad \sum_{\ell=-\infty}^{+\infty} (\delta_m^{\ell} - |\ell+\mu| \varepsilon_{\ell} T_m^{\ell}) Y_{\ell} = T_m^{m_0}, \quad m = 0, \pm 1, \pm 2, \dots$$

and

$$(33) \quad \sum_{\ell=-\infty}^{\infty} \left( \delta_m^\ell - \frac{1}{|\ell+\mu|} \eta_\ell W_m^\ell \right) x_\ell = W_m^{m_0}, \quad m = 0, \pm 1, \pm 2, \dots$$

where  $\delta_m^\ell$  is the Kronecker symbol and

$$(34) \quad T_m^\ell = \frac{1}{m+\mu} \left( V_m^\ell + \frac{1}{2} \frac{\mu}{\ell+\mu} P_m(u) (P_{\ell-1}(u) - P_\ell(u) \frac{P_\mu(u)}{P_{\mu-1}(u)}) \right)$$

and

$$(35) \quad W_m^\ell = (\ell+\mu) V_m^\ell + \frac{1}{2} \mu P_m(u) \left( P_{\ell-1}(u) + P_\ell(u) \frac{P_\mu(-u)}{P_{\mu-1}(-u)} \right)$$

with

$$(36) \quad V_m^\ell = \begin{cases} \frac{m}{m-\ell} \frac{1}{2} (P_\ell(u) P_{m-1}(u) - P_{\ell-1}(u) P_m(u)) & , \quad m \neq \ell \\ \frac{|m|}{m} \frac{1}{2} \sum_{n=1}^{|m|-1} \frac{P_n(u) (P_{n-1}(u) - P_{n+1}(u))}{2n+1} & , \quad m = \ell, \quad |\ell| > 0 \\ 0 & m = \ell = 0 \end{cases}$$

The infinite systems of equations for the  $x_\ell$  and  $y_\ell$  can be solved approximately by setting  $\epsilon_\ell = \eta_\ell = 0$  for  $|\ell| > M$ , where  $M > 0$  is a not too small integer. This yields a finite system for determining the  $x_\ell$  and  $y_\ell$ . Because of the fast convergence of the  $\epsilon_\ell = \eta_\ell = O(\ell^{-2})$  for  $|\ell| \rightarrow \infty$ , one gets a sufficiently good approximation for rather low values of  $M$ . Numerical tests showed that in most cases of interest  $M = 5$  did give excellent accuracy.

Calculating now the  $E_\varphi$  component at the ring position and inserting it in eq.(2), one gets the following expression for the coupling impedance:

A very useful approximation of the diagonal elements  $Z_{n,n}$  of the impedance can be derived for  $n/N \ll 1$  because it can then be

$$(37) \quad z_{N\ell+n,n} = \delta_{N\ell+n,n} z_n^{(r)} + z_{N\ell+n,n}^{(s)}$$

with

$$(38) \quad z_n^{(r)} = 4\pi^2 \int_0^\infty \left( \frac{n^2 k^2}{s^2 \omega^2} d_n(R,R) + \frac{\omega}{s^2} d'_n(R,R) \right) \frac{\sin^2 ka}{k^2 a^2} dk,$$

and

$$(39) \quad z_{N\ell+n,n}^{(s)} = -4\pi^2 \int_0^\infty \left( \frac{i\pi N(N\ell+n)nk^2}{\omega s^2} d_n(R,T) d_{N\ell+n}(R,T) x_{\ell+m_0} - \frac{i\pi\omega}{s^2 N} d'_n(R,T) d'_{N\ell+n}(R,T) y_{\ell+m_0} \right) \frac{\sin^2 ka}{k^2 a^2} dk,$$

where  $d_m, d'_m$  are combinations of Bessel and Hankel functions, defined by

$$(40) \quad d_m(r,r') = b_m(r,r') - \frac{b_m(r,P)b_m(r',P)}{b_m(P,P)},$$

$$d'_m(r,r') = b'_m(r,r') - \frac{b'_m(r,P)b'_m(r',P)}{b'_m(P,P)},$$

The  $b_m(r,r'), b'_m(r,r')$  are defined by eqs.(8), (9). The coefficients  $x_{\ell+m_0}, y_{\ell+m_0}$  are solutions of the eqs.(32), (33), which have to be determined for each value of  $k$  in the integrand of eq.(39). Furthermore, at  $k = \omega$  the integrand has a pole. As mentioned above, one has to add a small imaginary part  $\epsilon$  to the real  $\omega > 0$  to obtain the retarded solution for the electromagnetic field. From this it follows that one has to take the integration contour below the pole, as shown in Fig.2. The physical meaning of that pole contribution will be discussed later.



### III. Results and Approximations

Concerning the dependence of the impedance matrix  $Z_{N\ell+n,n}$  on the various parameters, we shall restrict discussion to the diagonal elements  $Z_{n,n}$ . The off-diagonal elements are small and, as far as the negative mass instability is concerned, they cause small corrections only to the growth rates as shown by Masunov [18], [12].

Furthermore, because the stability criterion [19] depends on the absolute value of the impedance, in most examples only  $|Z_{n,n}|$  is shown. From the dispersion relation it follows that the frequency  $\omega$  has to be taken as  $\omega = nv/R$ , where  $v = (1-1/\gamma^2)^{1/2}$  is the electron velocity ( $\gamma$  = relativistic factor).

In Fig.3 the impedance  $|Z_{n,n}|/n$  is plotted as a function of the mode number  $n$  for three different configurations: squirrel cage only (radius  $T = 1.22 R$ ), conducting cylinder only (radius  $P = 0.77 R$ ) and a combination of both. The number of strips is  $N = 19$  and the ratio of strips width to squirrel cage period is  $D/L = 0.5$ . For comparison, the ring impedance in free space is shown. The essential result is that one gets high impedance if a squirrel cage only is present. The impedance exceeds by far the ring impedance in free space for low mode numbers  $n$ . The main reason for this is the above-mentioned pole contribution at  $k = \omega$ , which is a TEM mode. If one considers the electromagnetic field produced by the electron ring perturbation, in terms of the transverse mode expansion, one gets, besides the TE and TM modes, a degenerate TEM mode at  $k = \omega$ . This TEM mode is a wave  $e^{i\omega(|z|-t)}$  propagating undamped along the squirrel cage and constitutes the main contribution to the real part of  $|Z_{n,n}|$ . This effect may be partly reduced for a squirrel cage of finite axial length. The impedance is considerably reduced by adding a coaxial cylinder. But even in that case the impedance is still larger than if only the cylinder were present.

A very useful approximation of the diagonal elements  $Z_{n,n}$  of the impedance can be derived for  $n/N \ll 1$  because it can then be

assumed that  $\epsilon_\ell = \eta_\ell = 0$  for  $|\ell| \geq 1$ , and so only  $\epsilon_0$  and  $\eta_0$  have to take into account. Solving eqs.(32) and (33), one gets for the coefficient  $x_0, y_0$

$$(41) \quad x_0 = \frac{\mu}{1 - \eta_0 - \mu \ln \frac{1-u}{2}},$$

$$y_0 = \frac{1}{\mu \left( 1 - \epsilon_0 - \frac{1}{\mu \ln \frac{1+u}{2}} \right)},$$

where use has been made the expansion of the Legendre function  $P_\mu(u)$  for  $|\mu| \ll 1$

$$(42) \quad P_\mu(u) = 1 + \mu \ln \frac{1+u}{2}.$$

Inserting  $x_0$  and  $y_0$  into the general formula (39), the squirrel cage contribution to the impedance becomes

$$(43) \quad Z_{n,n}^{(s)} = -4\pi^2 \int_0^\infty \left( \frac{n^2 k^2}{\omega s^2} \frac{d_n^2(R,T)}{d_n(T,T) - \frac{i}{N\pi} \ln \frac{1-u}{2}} + \right. \\ \left. + \frac{\omega}{s^2} \frac{d_n'^2(R,T)}{d_n'(T,T) - \frac{iN}{\pi \ln \frac{1+u}{2}}} \right) \frac{\sin^2 ka}{k^2 a^2} dk,$$

where  $u = \cos(\pi D/L)$  and  $s^2 = \omega^2 - k^2$ .

The dependence of  $Z_{n,n}$  on the number  $N$  and the width  $u$  of the strips becomes very simple in this approximation. In the limiting cases  $u = +1$  ( $D = 0$ ) and  $u = -1$  ( $D = L$ ) one obtains the impedance of one cylinder with radius  $T$  and of two concentric cylinders with radii  $T$  and  $P$ . Because of the logarithmic depen-

dence on  $u$ , the limiting cases are approached very slowly. In Figs.4 and 5 the impedance is shown as a function of the strip width  $D/L$ . It turns out that the impedance is almost constant for a wide range of the strip width.

In Figs.6 and 7 the dependence of  $Z_{n,n}$  on the number  $N$  of strips is shown for fixed  $u = 0$  and  $n = 4$ . For  $N \gg n$  the impedance increases with  $N$ . If  $N$  is comparable with or smaller than  $n$ , one gets a more complicated behaviour which depends sensitively on the geometry of the configuration. Taking the limit  $N = \infty$  for fixed  $u$  in eq.(41), one gets the impedance of an anisotropically conducting cylinder (infinite conductivity axially, no conductivity azimuthally) [11].

The electron ring is assumed to be infinitely thin in the radial direction and of finite length  $2a$  in the axial direction. The dependence of  $Z_{n,n}$  on the length  $2a$  is very weak. In all numerical examples shown here we chose  $a = 0.1 R$ . Concerning the dependence of  $Z_{n,n}$  on the mode number  $n$ , it has to be borne in mind that the stability criterion can be applied only for mode numbers  $nav/R < \pi$ , where the wavelength of the field perturbation is larger than the minor ring dimension because the variation of the fields over the ring cross-section is assumed to be small in deriving the criterion.

In Fig.8a-f the impedance of a ring inside or outside a squirrel cage of radius  $T$  is plotted as a function of  $T$  for different  $n$ . For higher  $n$  one gets very sharp resonances, which are less pronounced for wider slits. The impedance  $|Z_{n,n}|$  increases if the ring-to-squirrel-cage distance becomes smaller, which is mainly due to the increase of the real part of  $Z_{n,n}$ . This behaviour is in contrast to the case of a conducting cylinder, where the impedance gets smaller with decreasing distance of the ring to the wall. From all these results it can be concluded that if it is necessary to apply a squirrel cage for axial focussing one should add a conducting cylinder to keep the coupling impedance tolerably small.



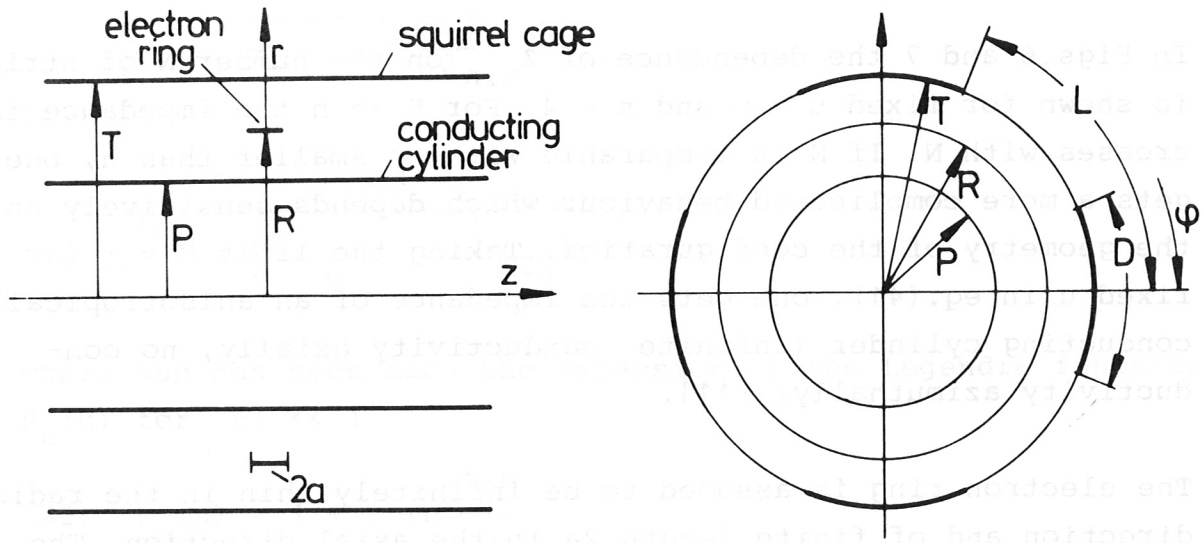


Figure 1: Schematic of squirrel cage configuration

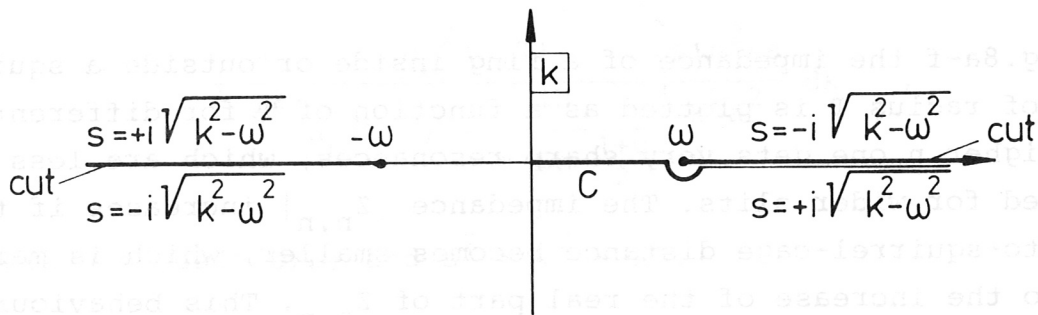


Figure 2: Complex k-plane, C contour of integration

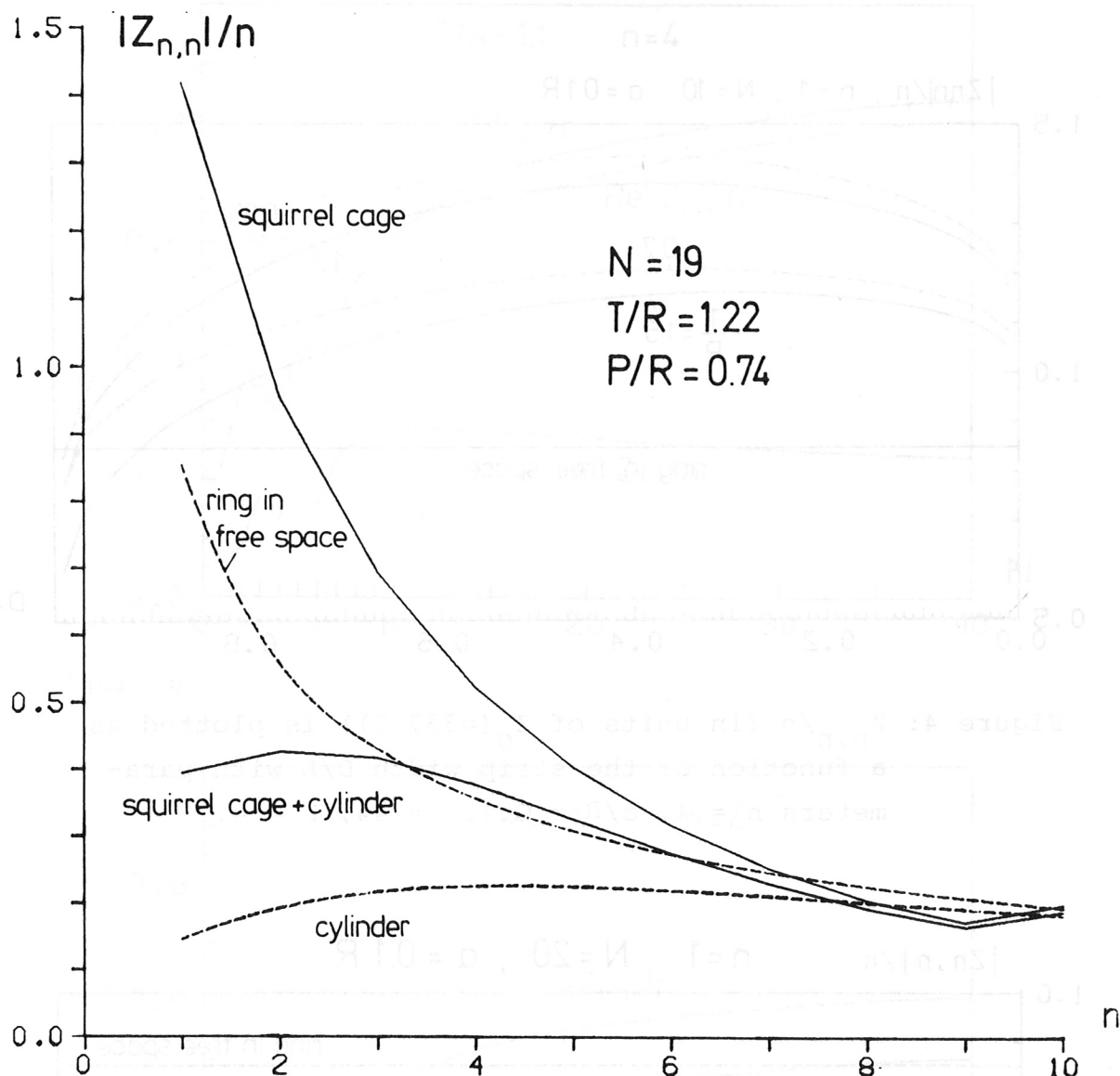


Figure 3: The impedance  $|Z_{n,n}|/n$  (in units of  $Z_0 (=377 \Omega)$ ) is plotted as a function of the mode number  $n$  for different configurations: squirrel cage only (radius  $T = 1.22 R$ ), cylinder only ( $P = 0.74 R$ ) and the combination of both. Number of strips  $N = 19$ , ratio of strip width to squirrel cage period  $D/L = 0.5$ , ring length  $2a/R = 0.2$  and relativistic factor  $\gamma = 44$ . For comparison the impedance of the ring in free space is shown.

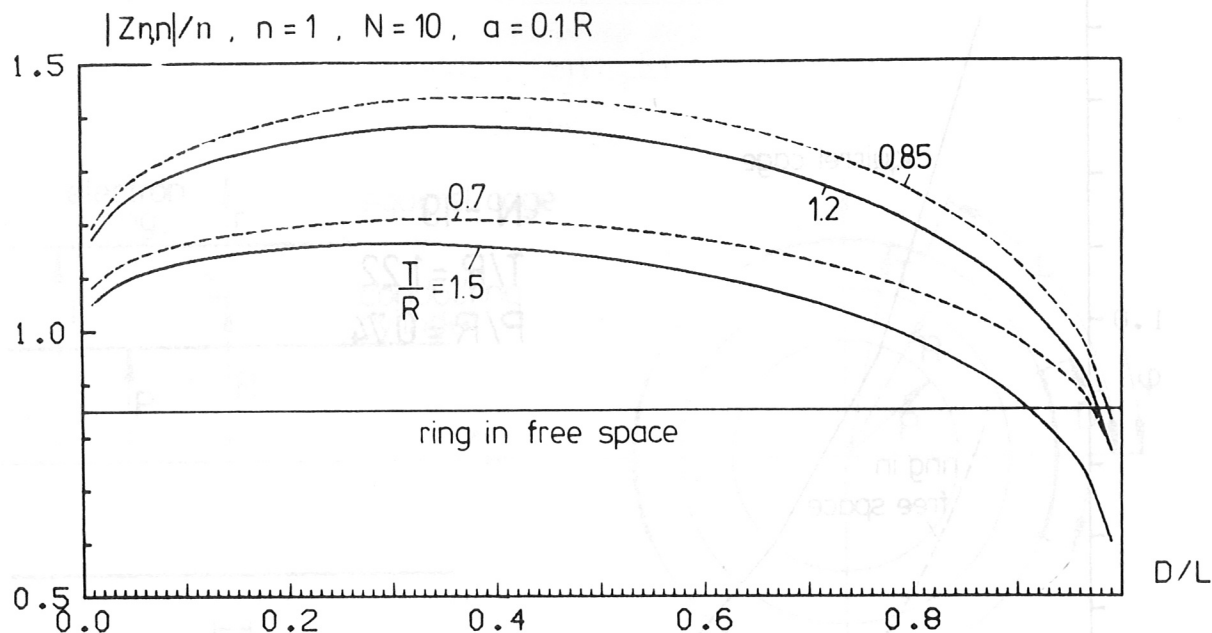


Figure 4:  $Z_{n,n}/n$  (in units of  $Z_0 (=337 \Omega)$ ) is plotted as a function of the strip width  $D/L$  with parameters  $n = 1$ ,  $a/R = 0.1$ ,  $\gamma = 44$ ,  $P = \infty$ .

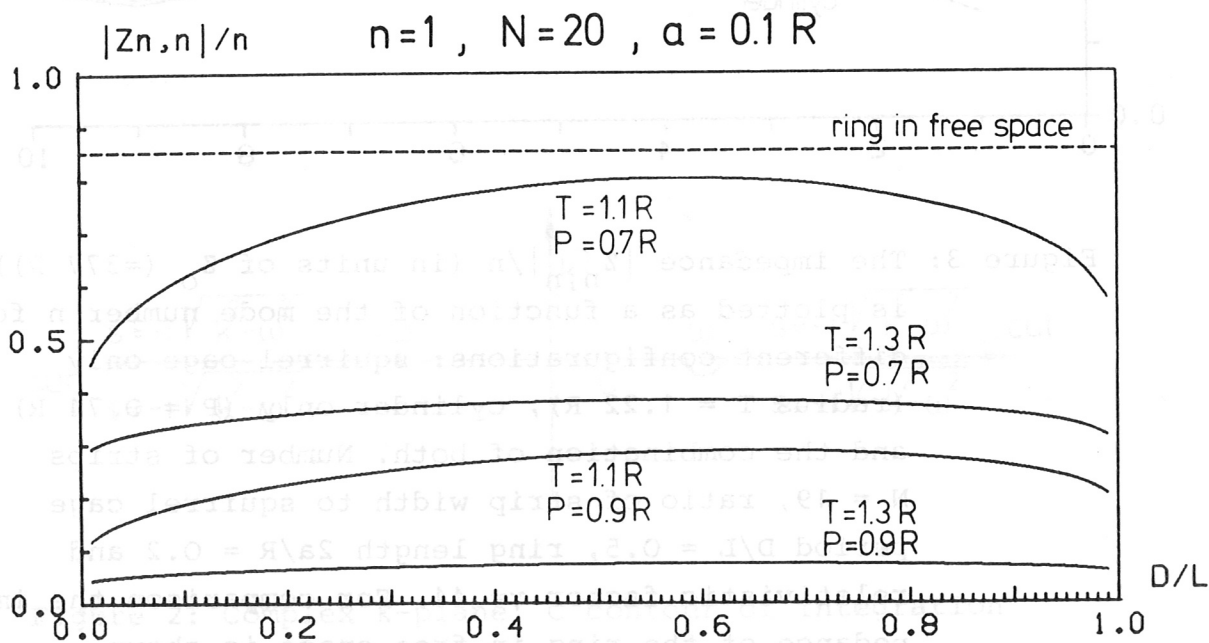


Figure 5:  $Z_{n,n}/n$  (in units of  $Z_0 (=377 \Omega)$ ) is plotted as a function of the strip width  $D/L$  with parameters  $n = 1$ ,  $a/R = 0.1$ ,  $\gamma = 44$ .



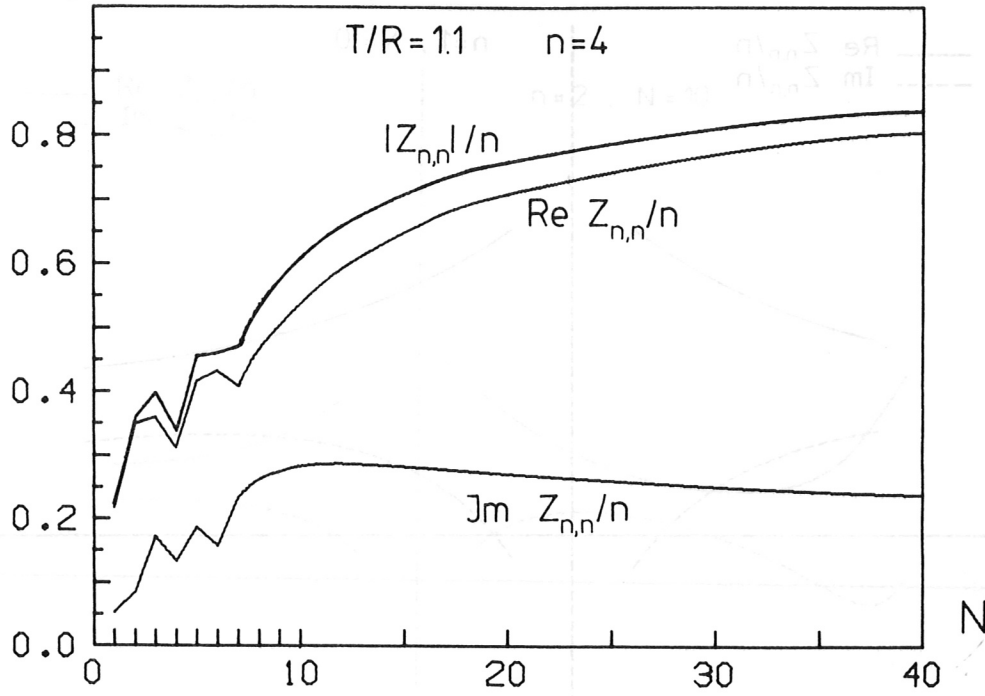


Figure 6

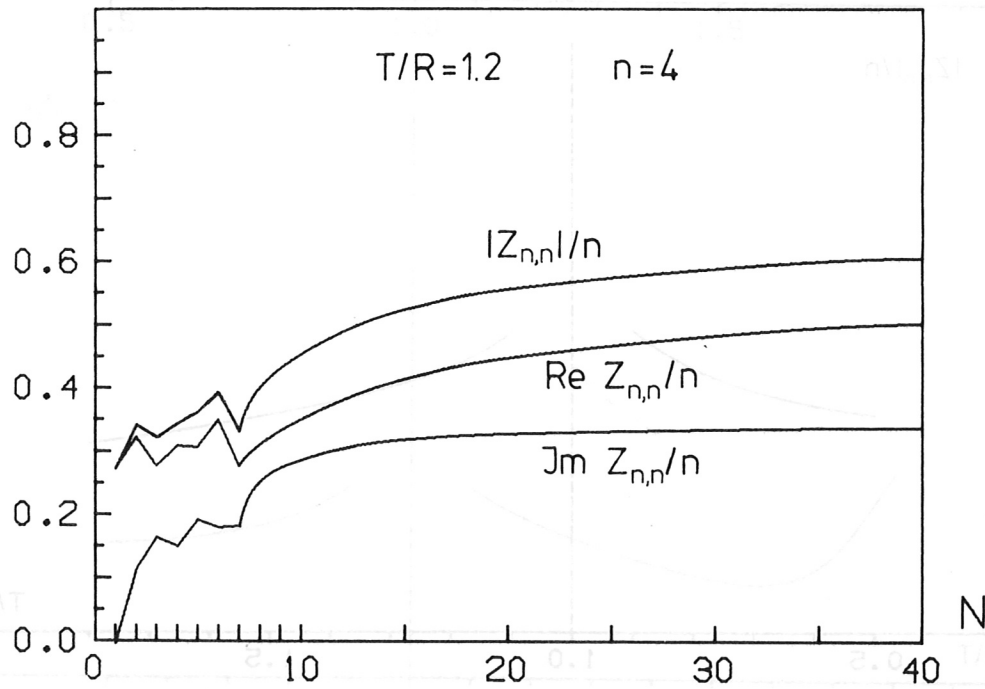


Figure 7

Figure 6 and 7:  $Z_{n,n}/n$  (in units of  $Z_0$  ( $=377 \Omega$ )) is plotted as a function of the number of strips  $N$  with parameters  $D/L = 0.5$ ,  $n = 4$ ,  $a/R = 0.1$ ,  $\gamma = 44$ ,  $P = \infty$ .

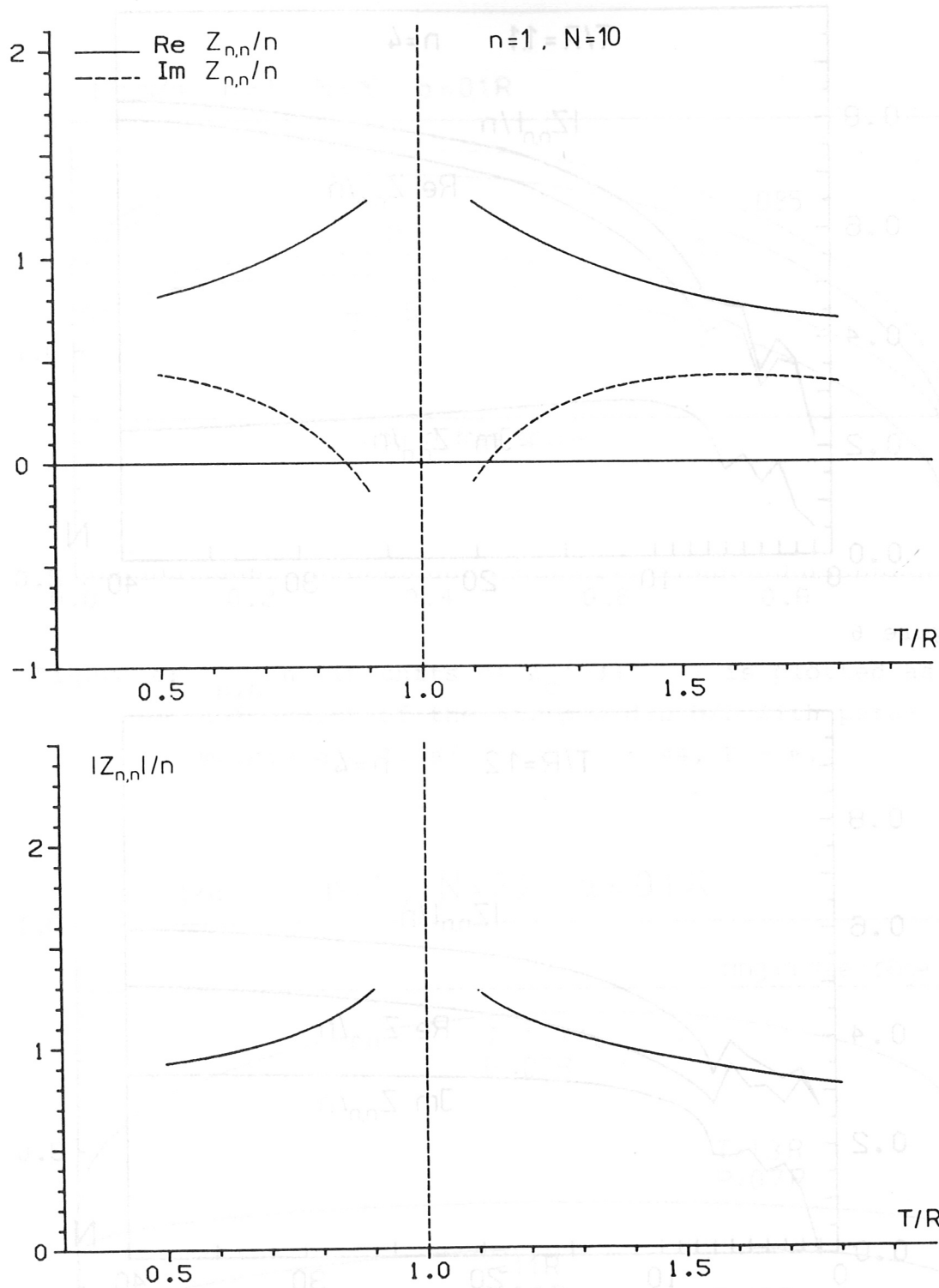


Figure 8a

Figures 8a-f:  $Z_{n,n}/n$  (in units of  $Z_0 (=377 \Omega)$ ) is plotted as a function of the squirrel cage radius  $T$  for different mode numbers  $n$  with parameters  $N = 10$ ,  $D/L = 0.85$ ,  $a/R = 0.1$ ,  $\gamma = 44$ ,  $P = \infty$ .

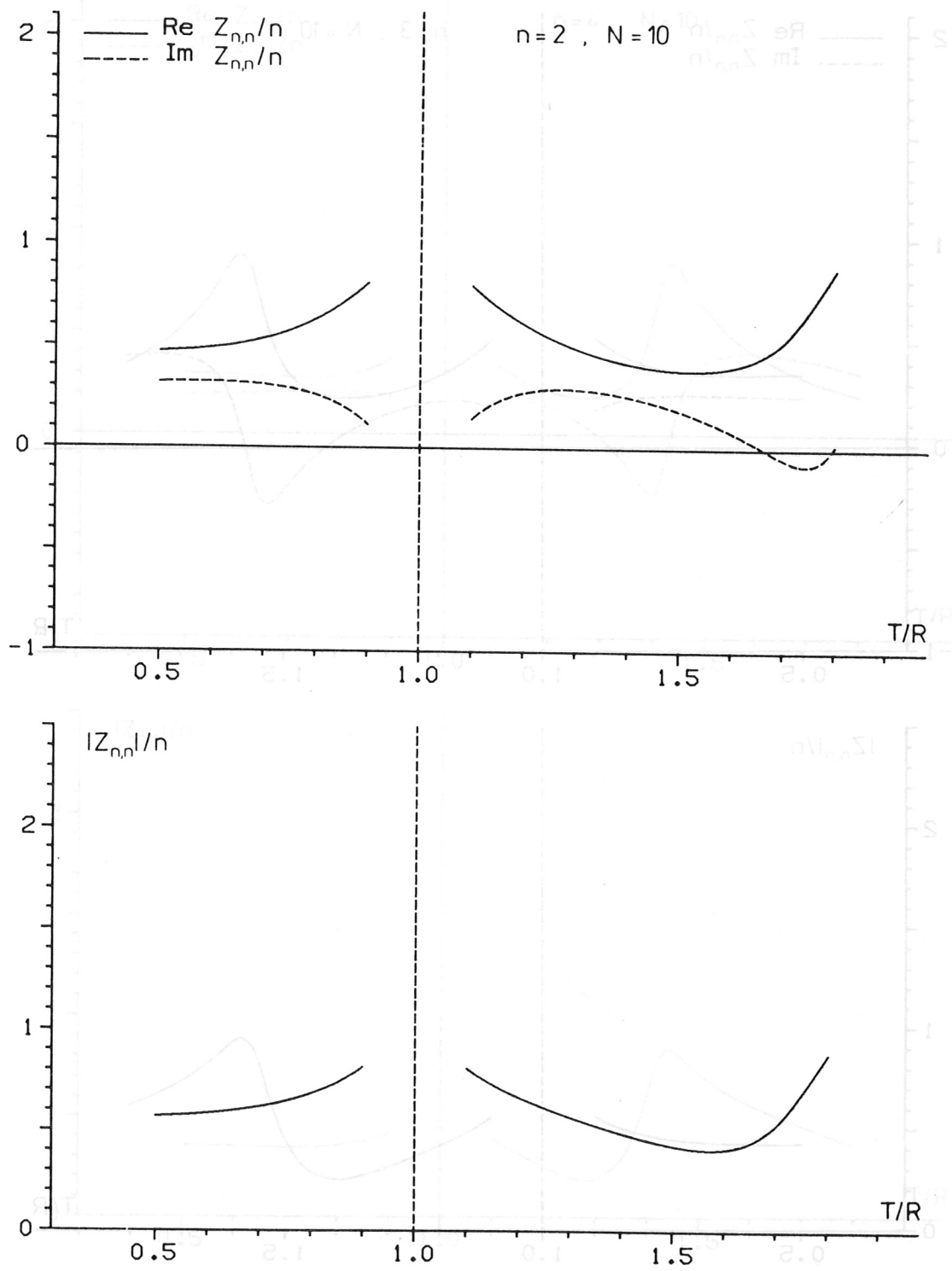


Figure 8b:

Figure 8c:

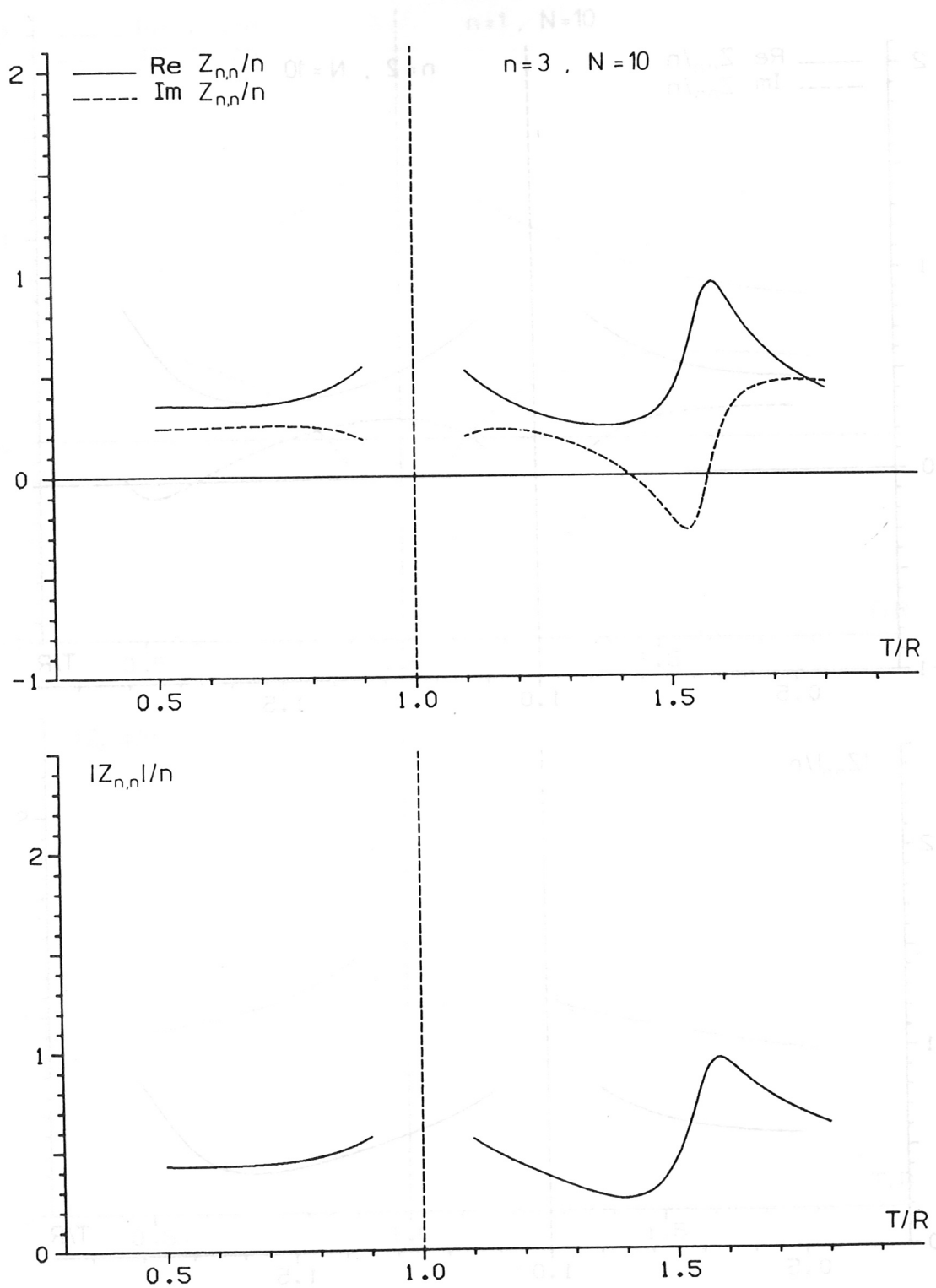


Figure 8c:

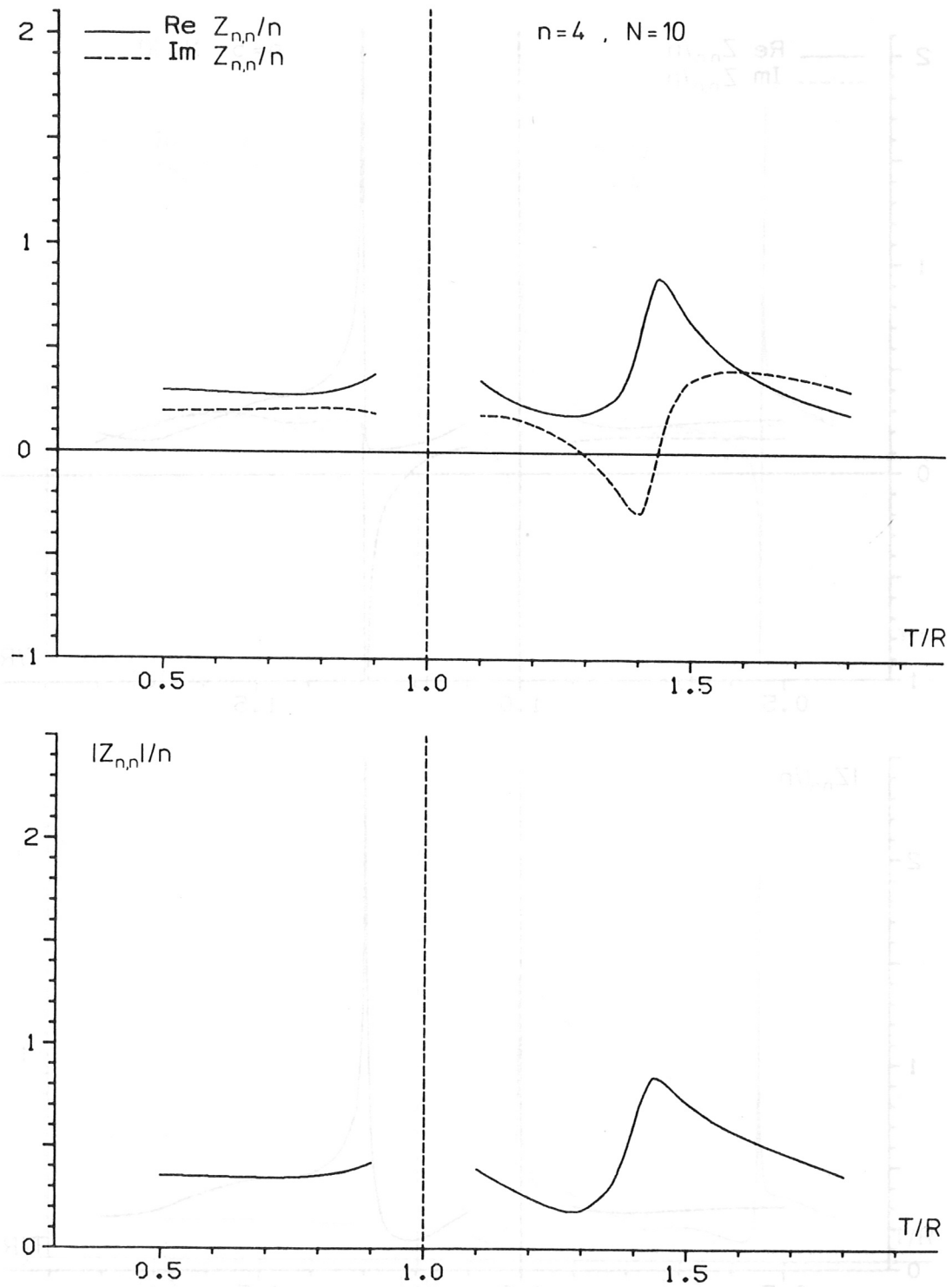


Figure 8d:



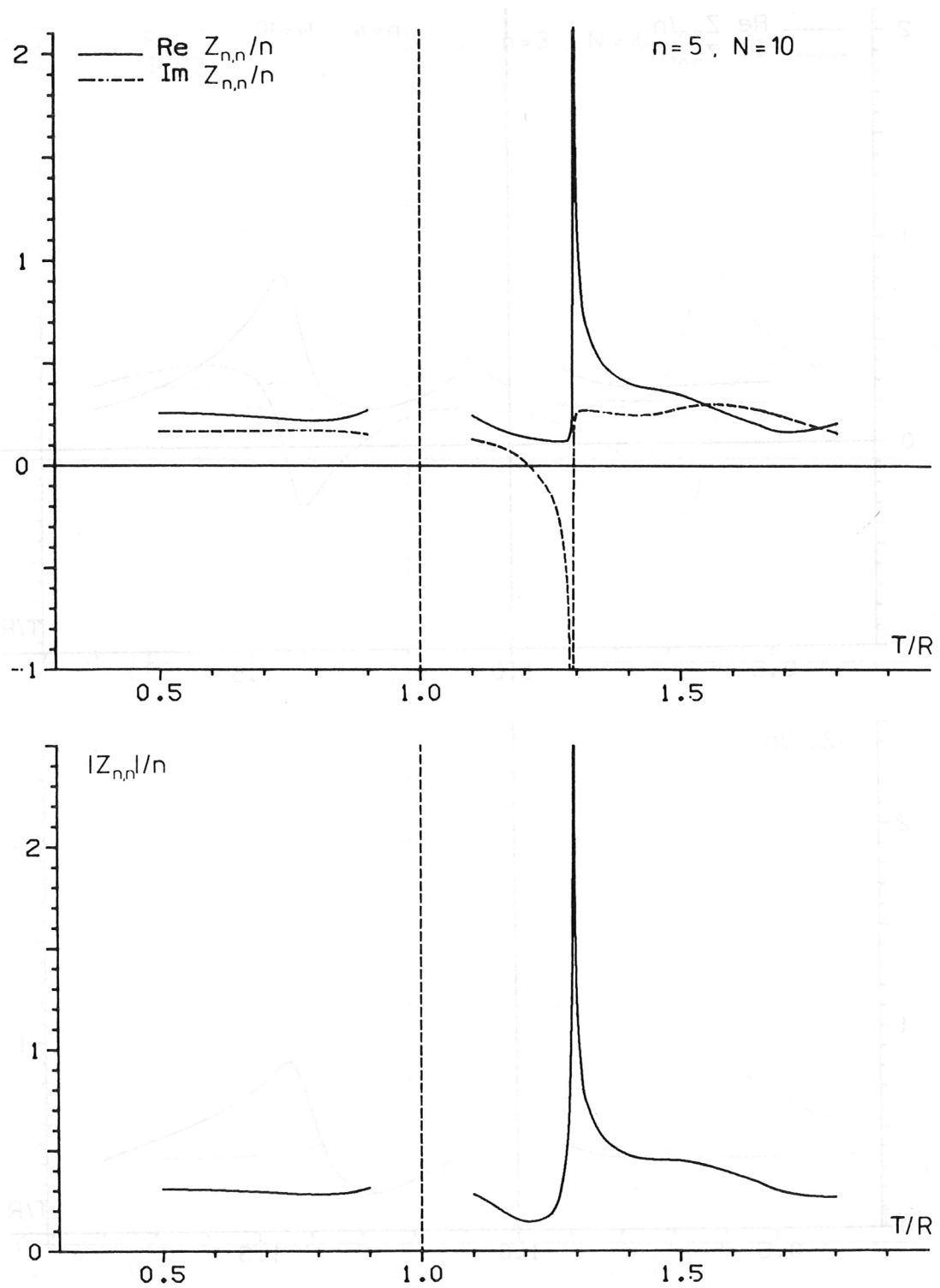


Figure 8e:

# Acknowledgements

The author would like to thank E. Springmann for carrying out the numerical calculations and W. Herrmann for his discussions.

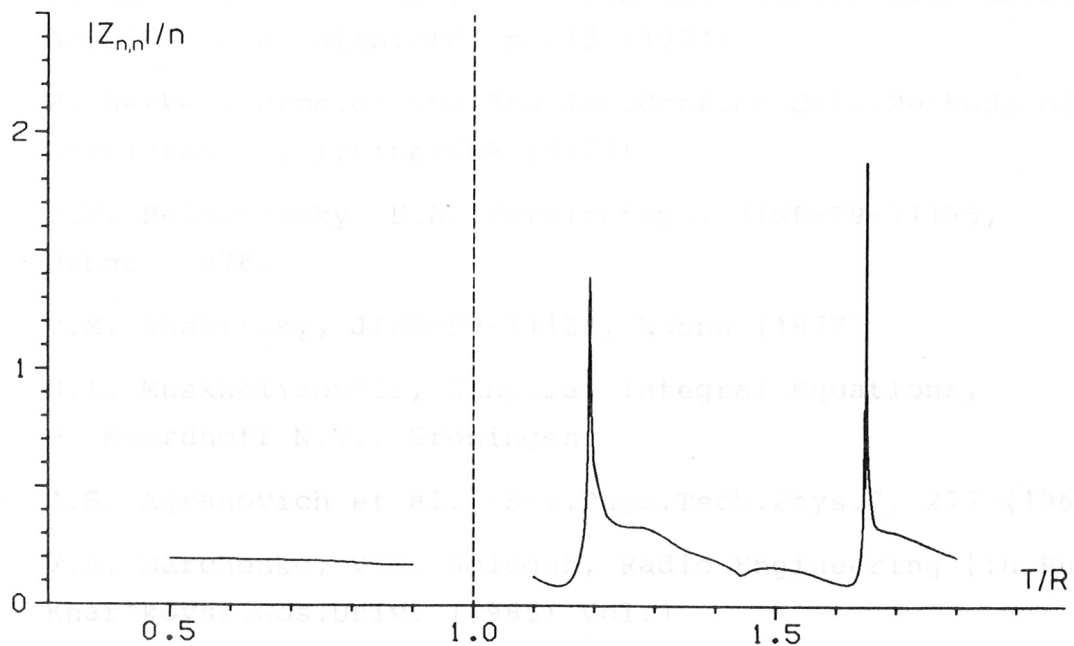
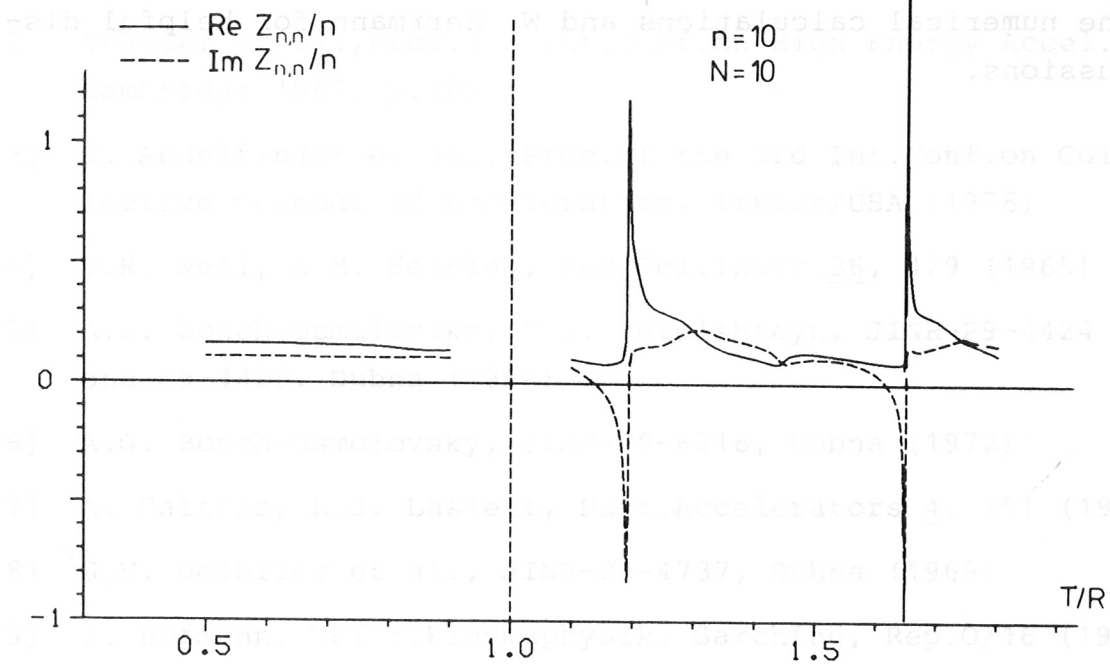


Figure 8f:

- [17] W. Magnus, F. Oberhettinger, R.P. Soni, Formulas and Theorems for the Special Functions of Mathem.Phys., Springer-Verlag, Berlin-Heidelberg-New York (1966)
- [18] E.S. Masunov, Sov.Phys.Tech.Phys.19, 1185 (1975)
- [19] L.J. Laslett, IEEE Trans.NS-20, 271 (1973)

### Acknowledgements

The author would like to thank E. Springmann for carrying out the numerical calculations and W. Herrmann for helpful discussions.

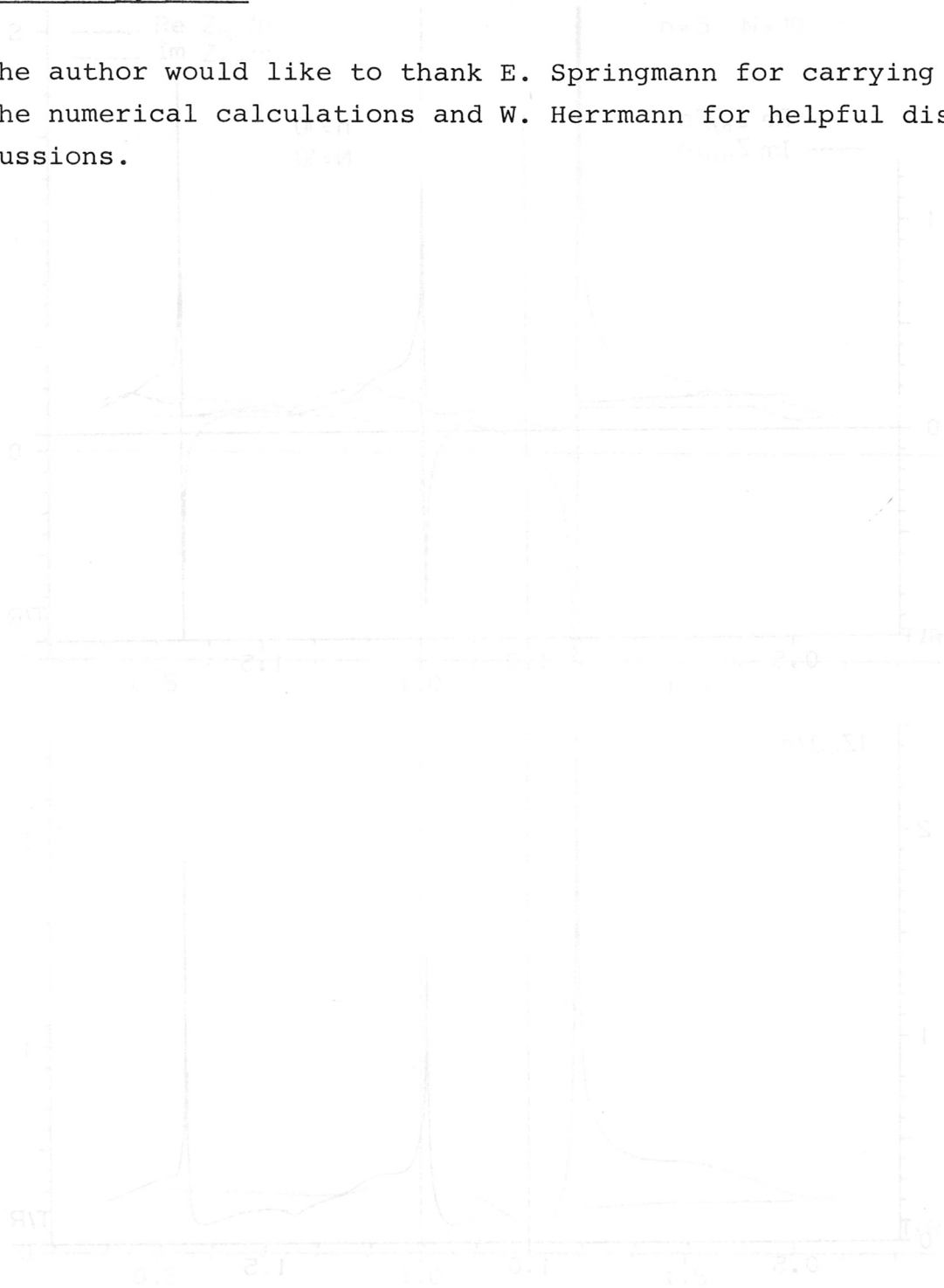


Figure 8a:

Figure 8b:

## References

- [ 1] C. Andelfinger et al., Proc.of the 1979 Part.Accel.Conf., San Francisco/USA
- [ 2] Veksler et al., Proc.4th Int.Conf.on High Energy Accel., Cambridge 1967, p.289
- [ 3] C. Andelfinger et al., Proc.of the 3rd Int.Conf.on Collective Methods of Acceleration, Irvine/USA (1978)
- [ 4] V.K. Neil, A.M. Sessler, Rev.Sci.Instr.36, 429 (1965)
- [ 5] A.G. Bonch-Osmolovsky, E.A. Perelshteyn, JINR-P9-4424 and P9-4425, Dubna (1969)
- [ 6] A.G. Bonch-Osmolovsky, JINR-P9-6318, Dubna (1972)
- [ 7] A. Faltens, L.J. Laslett, Part.Accelerators 4, 151 (1973)
- [ 8] G.V. Dolbilov et al., JINR-P9-4737, Dubna (1969)
- [ 9] I. Hofmann, MPI f.Plasmaphysik, Garching, Rep.O/16 (1973)
- [10] C. Andelfinger et al., Proc.9th Int.Conf.on High Energy Accelerators, Stanford, p.218 (1974)
- [11] P. Merkel, Proc.of the 3rd Int.Conf.on Coll.Methods of Acceleration, Irvine/USA (1978)
- [12] P.F. Beloshitsky, E.A. Perelshteyn, JINR-P9-11195, Dubna (1978)
- [13] V.M. Zhabitsky, JINR-P9-11123, Dubna (1977)
- [14] N.I. Muskhelishvili, Singular Integral Equations, P. Noordhoff N.V., Groningen
- [15] Z.S. Agranovich et al., Sov.Phys.Tech.Phys.7, 277 (1962)
- [16] V.A. Marchenko, V.G. Sologub, Radio Engineering [in Russian] Khar'kovsk.Gos.Univ. (1965) Vol.1
- [17] W. Magnus, F. Oberhettinger, R.P. Soni, Formulas and Theorems for the Special Functions of Mathem.Phys., Springer-Verlag, Berlin-Heidelberg-New York (1966)
- [18] E.S. Masunov, Sov.Phys.Tech.Phys.19, 1185 (1975)
- [19] L.J. Laslett, IEEE Trans.NS-20, 271 (1973)

## Appendix

In this section we derive the solution of three auxiliary systems of equations for solving eqs. (28)-(31). These problems are special cases of the Hilbert problem. The general theory of the Hilbert problem is extensively treated in the book of Mushkelishvili [14].

The problems discussed here are solved by Agronovich et al. [15] and by Marchenko and Sologub [16]. In the following a derivation of the solutions will be given using generating functions.

### 1. Problem

We start by considering the system of equations

$$(A1) \quad \sum_{n=-\infty}^{\infty} x_n e^{in\varphi} = 0, \quad \varphi_0 < |\varphi| < \pi$$

$$\sum_{n=-\infty}^{\infty} \frac{|n|}{n} x_n e^{in\varphi} = \sum_{n=-\infty}^{\infty} f_n e^{in\varphi}, \quad |\varphi| < \varphi_0,$$

where  $\frac{|n|}{n} = 1$  for  $n \neq 0$ . The function on the right side of the second equation, written as a Fourier sum, is given. The coefficients  $x_n$  are to be determined.

One defines the following functions in the complex  $z$ -plane:

$$(A2) \quad x^+(z) = \sum_{n=1}^{\infty} x_n z^n, \quad x^-(z) = - \sum_{n=0}^{-\infty} x_n z^n.$$

The function  $x^+(z)$  is holomorphic for  $|z| < 1$  and  $x^-(z)$  is holomorphic for  $|z| > 1$ .



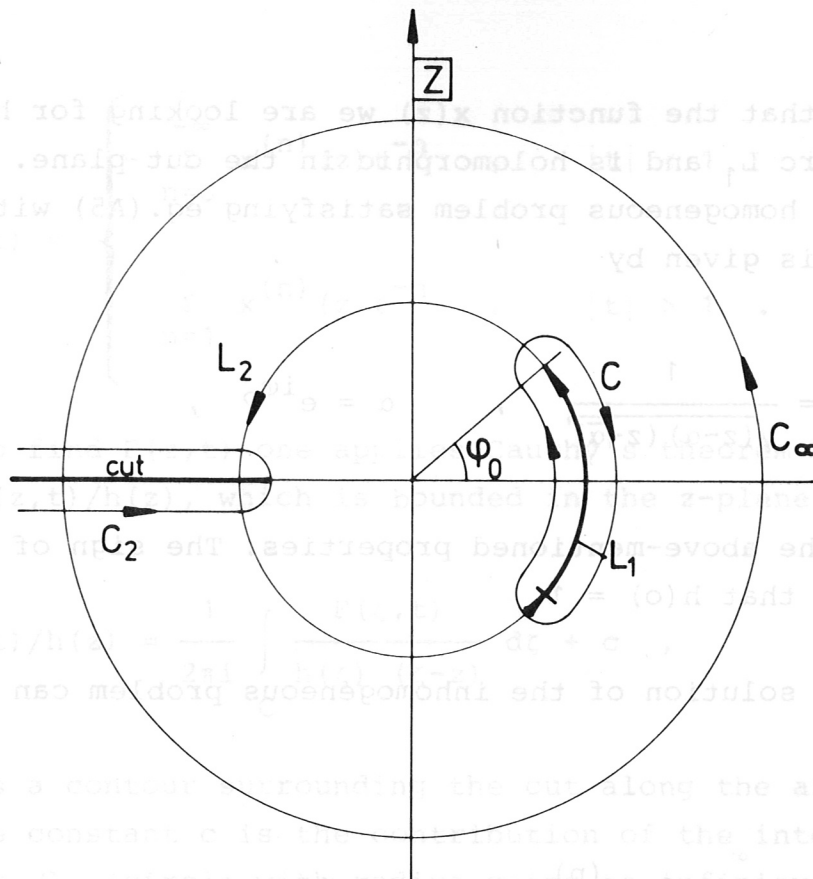


Fig.A1 Complex \$z\$ plane

From eq.(A1) it follows that

$$(A3) \quad x^+(e^{i\varphi}) - x^-(e^{i\varphi}) = 0, \quad \text{for } \varphi_0 < |\varphi| < \pi.$$

The functions \$x^+(z)\$ and \$x^-(z)\$ coincide on the arc \$L\_2\$ (see Fig.A1). Therefore, \$x^+(z)\$ and \$x^-(z)\$ are the same analytical function \$x(z)\$:

$$(A4) \quad x(z) = \begin{cases} x^+(z), & |z| < 1, \\ x^-(z), & |z| > 1. \end{cases}$$

On the arc \$L\_1\$ it holds that

$$(A5) \quad x^+(e^{i\varphi}) + x^-(e^{i\varphi}) = \sum_{n=-\infty}^{+\infty} f_n e^{in\varphi}, \quad |\varphi| < \varphi_0.$$

The problem thus consists of determining a sectionally holomorphic function \$x(z)\$ from the sum of the limiting values of \$x(z)\$ on the arc \$L\_1\$ inside and outside the unit circle.

This means that the function  $x(z)$  we are looking for has a cut along the arc  $L_1$  and is holomorphic in the cut plane. The solution of the homogeneous problem satisfying eq.(A5) with vanishing right side is given by

$$(A6) \quad h(z) = \frac{1}{\sqrt{(z-\alpha)(z-\bar{\alpha})}} \quad , \quad \alpha = e^{i\varphi_0} \quad ,$$

which has the above-mentioned properties. The sign of the root is chosen such that  $h(0) = 1$ .

The general solution of the inhomogeneous problem can be written as

$$(A7) \quad x(z) = \sum_{n=-\infty}^{\infty} f_n x^{(n)}(z) + a h(z) \quad ,$$

where  $x^{(n)}(z)$  is a solution of the inhomogeneous problem with the inhomogeneous term  $e^{in\varphi}$ , and where  $a$  is an arbitrary constant. Without loss of generality one can require that  $x^{(n)}(0) = 0$ , because one can add to  $x^{(n)}(z)$  an arbitrary homogeneous solution.

An elegant way of finding  $x^{(n)}(z)$  is to solve the special inhomogeneous problem taking as inhomogeneous term in eq.(A5) the function

$$(A8) \quad f(\varphi, t) = \frac{e^{i\varphi}}{t - e^{i\varphi}} \quad ,$$

which depends on a parameter  $t$ . Expanding  $f(\varphi, t)$  in a power series of  $t$ , for  $|t| < 1$  and  $|t| > 1$ , the coefficients of  $t^{-n}$  are the  $e^{in\varphi}$ . Letting  $F(z, t)$  now be the solution of eq.(A5) with the inhomogeneous term (A8), it then follows that the  $x^{(n)}(z)$  are the coefficients of the  $t$ -expansion of  $F(z, t)$ . It holds that

$$(A9) \quad F(z, t) = \begin{cases} - \sum_{n=0}^{\infty} x^{(n)}(z) t^{-n} & , \quad |t| < 1 \\ \sum_{n=1}^{\infty} x^{(n)}(z) t^{-n} & , \quad |t| > 1 \end{cases}$$

In order to find  $F(z, t)$  one applies Cauchy's theorem to the function  $F(z, t)/h(z)$ , which is bounded in the  $z$ -plane. One gets

$$(A10) \quad F(z, t)/h(z) = \frac{1}{2\pi i} \int_C \frac{F(\zeta, t)}{h(\zeta) (\zeta - z)} d\zeta + c ,$$

where  $C$  is a contour surrounding the cut along the arc  $L_1$  (see Fig.1). The constant  $c$  is the contribution of the integral along the contour  $C_\infty$  (circle with radius going to infinity). Contracting the contour  $C$  on the cut and taking into account the different signs of the limiting values of the square root  $h(\zeta)$  at the cut, the integral becomes

$$(A11) \quad F(z, t)/h(z) = \frac{1}{2\pi i} \int_{L_1} \frac{(F^+(\zeta, t) + F^-(\zeta, t)) \sqrt{(\zeta - \alpha)(\zeta - \bar{\alpha})}}{\zeta - z} d\zeta + c ,$$

where the integration path is the oriented arc  $L_1$  inside the unit circle along the cut and where  $F^+(z, t)$  and  $F^-(z, t)$  are the function  $F(z, t)$  for  $|z| < 1$  and  $|z| > 1$  corresponding to the definition (A4). From the requirement  $F(0, t) = 0$ , which follows from  $x^{(n)}(0) = 0$ ,  $c$  can be determined:

$$(A12) \quad c = - \frac{1}{2\pi i} \int_{L_1} \frac{(F^+(\zeta, t) + F^-(\zeta, t)) \sqrt{(\zeta - \alpha)(\zeta - \bar{\alpha})}}{\zeta} d\zeta .$$

Inserting eq.(A5) with eq.(A8) in (A11) and using eq.(A12), one now obtains

$$(A13) \quad F(z, t) = \frac{z}{\sqrt{(z-\alpha)(z-\bar{\alpha})}} \frac{1}{2\pi i} \int_{L_1} d\zeta \frac{\sqrt{(\zeta-\alpha)(\zeta-\bar{\alpha})}}{(t-\zeta)(\zeta-z)}.$$

The integral can be carried out using Cauchy's theorem and one gets for the "generating" function

$$(A14) \quad F(z, t) = \frac{1}{2} \left( \frac{z}{t-z} - \frac{z}{t-z} \frac{\sqrt{t^2-2ut+1}}{\sqrt{z^2-2uz+1}} - \frac{z}{\sqrt{z^2-2uz+1}} \right),$$

where  $u = (\alpha + \bar{\alpha})/2 = \cos \varphi_0$ . The generating function is sectionally holomorphic and has a cut along the arc  $L_1$  in the  $z$ -plane as well as in the  $t$ -plane.

Expanding  $F(z, t)$  in a power series of  $t$  and  $z$  the unknown coefficients  $x_n$  can be expressed in terms of the expansion coefficients. One has to distinguish four different regions

$$(A15) \quad F(z, t) = \begin{cases} \sum_{n=1, m=1}^{\infty, \infty} V_m^n t^{-n} z^m, & |t| > 1, |z| < 1, \\ - \sum_{n=1, m=0}^{\infty, -\infty} V_m^n t^{-n} z^m, & |t| > 1, |z| > 1, \\ - \sum_{n=0, m=1}^{-\infty, \infty} V_m^n t^{-n} z^m, & |t| < 1, |z| < 1, \\ \sum_{n=0, m=0}^{-\infty, -\infty} V_m^n t^{-n} z^m, & |t| < 1, |z| > 1. \end{cases}$$

Using the expansion of the function  $h(z)$  in terms of the Legendre polynomials  $P_\ell(u)$

$$(A16) \quad \frac{1}{\sqrt{z^2 - 2uz + 1}} = \begin{cases} \sum_{\ell=0}^{\infty} P_\ell(u) z^\ell, & |z| < 1 \\ -\sum_{\ell=0}^{\infty} P_\ell(u) z^{-\ell-1}, & |z| > 1 \end{cases}$$

the expansion coefficients  $V_m^n$  of  $F(z, t)$  are found to be

$$(A17) \quad V_m^n = \begin{cases} \frac{m}{m-n} \frac{1}{2} (P_n(u) P_{m-1}(u) - P_{n-1}(u) P_m(u)), & n \neq m \\ \frac{|n|}{n} \frac{1}{2} \sum_{\ell=0}^{|n|-1} \frac{P_\ell(u) (P_{\ell-1}(u) - P_{\ell+1}(u))}{2\ell+1}, & n = m, |n| > 0 \\ 0, & n = m = 0 \end{cases}$$

From eqs. (A9), (A7) and (A2) it follows by comparison that the coefficients  $x_m$  are given by

$$(A18) \quad x_m = \sum_{n=-\infty}^{+\infty} V_m^n f_n + a P_m(u), \quad m = 0, \pm 1, \pm 2, \dots$$

This is the general solution of the problem (A1), where the  $V_m^n$  are given by eq. (A17),  $P_m(u)$  are the Legendre polynomials and  $a$  is an arbitrary constant.



## 2. Problem

The second problem we consider is the system of equations

$$(A19) \quad \sum_{n=-\infty}^{+\infty} y_n e^{in\varphi} = 0, \quad \varphi_0 < |\varphi| < \pi$$

$$\sum_{n=-\infty}^{+\infty} |n+\mu| y_n e^{in\varphi} = \sum_{n=-\infty}^{+\infty} f_n e^{in\varphi}, \quad \varphi_0 > |\varphi|,$$

where  $0 \leq \mu < 1$ . To solve this set of equations, we define the following sectionally holomorphic functions as in the previous case

$$(A20) \quad y^+(z) = \sum_{n=1}^{\infty} y_n z^n, \quad |z| < 1, \quad y^-(z) = \sum_{n=0}^{-\infty} y_n z^n, \quad |z| > 1.$$

Because of the first eq. (A19) the functions  $y^+(z)$ ,  $y^-(z)$  are the same sectionally holomorphic function, coinciding along the arc  $L_2$ :

$$(A21) \quad y(z) = \begin{cases} y^+(z), & |z| < 1, \\ y^-(z), & |z| > 1. \end{cases}$$

We now define the function  $g(z)$  by

$$(A22) \quad g(z) := z \frac{d}{dz} y(z) + \mu y(z).$$

Because of eq. (21) the function  $g(z)$  is also sectionally holomorphic. From the second eq. (A19) it follows that along the arc  $L_1$  it holds that

$$(A23) \quad g^+(e^{i\varphi}) + g^-(e^{i\varphi}) = \sum_{n=-\infty}^{+\infty} f_n e^{in\varphi} \quad \text{for } \varphi_0 > |\varphi|,$$

where we have defined  $g^+(z)$  and  $g^-(z)$  corresponding to eq.(A21) as the function  $g(z)$  for  $|z| < 1$  and  $|z| > 1$  respectively.

This equation coincides with eq.(A5). The function  $g(z)$  is therefore the solution  $x(z)$  of the previously treated case. The general generating function for  $g(z)$  is thus

$$(A24) \quad G(z, t) = F(z, t) + \frac{a(t)}{\sqrt{z^2 - 2uz + 1}}.$$

To the special inhomogeneous solution  $F(z, t)$  we have added the general homogeneous solution. This is necessary because, unlike in the previous case, the solution  $g(z)$  is unique. As we shall see, the function  $a(t)$  is determined by the requirement that  $y(z) \approx z^{-1}$  for  $|z| \rightarrow \infty$ , which follows from eq.(A20). This can be seen by integrating eq.(A22):

$$(A25) \quad z^\mu y(z) - z_0^\mu y(z_0) = \int_{z_0}^z \zeta^{\mu-1} g(\zeta) d\zeta,$$

where  $z, z_0$  are the end points of the integration path  $C_2$ . The functions  $z^{\mu-1}g(z)$  and  $z^\mu y(z)$  have a cut along the negative real axis. Taking now the integration path  $C_2$  (see Fig.A1) around this cut, below and above the negative real axis, the right side has to vanish because of the requirement  $y(z) \approx z^{-1}$  for  $|z| \rightarrow \infty$ . One therefore gets the condition for  $g(z)$

$$(A26) \quad 0 = \int_{C_2} \zeta^{\mu-1} g(\zeta) d\zeta.$$

This condition, which also has to be satisfied by the generating function  $G(z, t)$ , determines the coefficient  $a(t)$  of the homogeneous solution. For the evaluation it is convenient to shift the contour  $C_2$ . The function  $G(z, t)z^{\mu-1}$  has cuts along the negative real axis and along the arc  $L_1$ . Shifting the contour  $C_2$

to the contour  $C$ , around the arc  $L_1$  and contracting it on the arc  $L_1$ , we get for  $a(t)$  with eq.(A14) and eq.(A24)

$$(A27) \quad a(t) \int_{L_1} \frac{\zeta^{\mu-1} d\zeta}{\sqrt{\zeta^2 - 2u\zeta + 1}} = + \frac{1}{2} \int_{L_1} \frac{\zeta^{\mu}}{\sqrt{\zeta^2 - 2u\zeta + 1}} \left( 1 + \frac{\sqrt{t^2 - 2ut + 1}}{t - \varphi} \right) d\zeta.$$

The integration path is the oriented arc  $L_1$  inside the unit circle along the cut.

One now introduces the Legendre function  $P_{\mu}(u)$  by the definition

$$(A28) \quad P_{\mu}(u) = \frac{1}{i\pi} \int_{L_1} \frac{\zeta^{\mu} d\zeta}{\sqrt{\zeta^2 - 2u\zeta + 1}},$$

where the integration contour is along the oriented arc  $L_1: = \{\zeta = e^{+i\varphi}, -\varphi_0 \leq \varphi \leq \varphi_0\}$ ,  $u = \cos \varphi_0$ . Using this definition, the integrals in eq.(A26) can be evaluated by expanding  $a(t)$  in a power series:

$$(A29) \quad a(t) = \begin{cases} -\sum_{n=0}^{\infty} a_n t^{-n} & , \quad |t| < 1, \\ +\sum_{n=1}^{\infty} a_n t^{-n} & , \quad |t| > 1, \end{cases}$$

where the coefficients  $a_n$  are given by

$$(A30) \quad a_n = \frac{\mu}{n+\mu} \frac{1}{2P_{\mu-1}(u)} (P_{n-1}(u) P_{\mu-1}(u) - P_n(u) P_{\mu}(u)).$$

To obtain the unknown coefficients  $y_n$ , one expands the function  $G(t)$  in a double power series in  $t$  and  $z$ . With eqs.(A15), (A16) and (A18) one gets

$$(A31) \quad G(z, t) = \pm \sum_{n, m} (V_m^n + a_n P_m) t^{-n} z^m, \quad \text{This problem can be treated in terms of the new variables and coefficients}$$

where the prescriptions for the summation and the sign are exactly the same as in eq.(A15).

Finally, inserting  $G(z, t)$  in eq.(A22), one gets the  $y_m$

$$(A32) \quad y_m = \sum_{n=-\infty}^{+\infty} T_m^n f_n \quad \text{Eq. (A32) in terms of the new quantities}$$

with

$$(A33) \quad T_m^n = \frac{1}{m+\mu} (V_m^n + a_n P_m(u)), \quad \text{(A33)}$$

where the  $V_m^n$  given by eq.(A15) and the  $a_n$  by eq.(A30).

The equations for  $y_n$  are solved assuming  $\mu \neq 0$ . But the limiting case  $\mu = 0$  is also included in the solution. The only matrix elements  $T_m^n$  whose definition may be doubtful are the  $T_0^n$ . For them one gets for  $\mu = 0$

$$T_0^n = - \frac{1}{2n} (P_n(u) - P_{n-1}(u)), \quad n \neq 0 \quad \text{(A34)}$$

$$T_0^0 = - \ln \frac{1+u}{2} \quad \text{with}$$

### 3. Problem Using the property of the Legendre function $P(u)$

The last system of equations we consider is given by

$$(A35) \quad \sum_{n=-\infty}^{+\infty} x_n e^{in\varphi} = 0, \quad \varphi_0 < |\varphi| < \pi$$

$$\sum_{n=-\infty}^{+\infty} \frac{1}{|n+\mu|} x_n e^{in\varphi} = \sum_{n=-\infty}^{+\infty} g_n e^{in\varphi}, \quad \varphi_0 > |\varphi|.$$

This problem can be transformed to the 2nd problem. Introducing new variables and coefficients

$$\begin{aligned} \varphi' &= \varphi - \pi, \\ (A36) \quad y_n &= \left( \frac{x_n}{|n+\mu|} - g_n \right) (-1)^n, \\ \varphi_1 &= \pi - \varphi_0, \end{aligned}$$

Eqs.(A35) in terms of the new quantities are then

$$\begin{aligned} (A37) \quad \sum_{n=-\infty}^{+\infty} y_n e^{in\varphi'} &= 0, \quad \varphi_1 < |\varphi'| < \pi \\ \sum_{n=-\infty}^{+\infty} |n+\mu| y_n e^{in\varphi'} &= \sum_{n=-\infty}^{+\infty} (-1)^{n-1} g_n |n+\mu| e^{in\varphi'}, \quad \varphi_1 > |\varphi'|, \end{aligned}$$

where  $\cos \varphi_1 = -\cos \varphi_0 = -u$ . The solution of these equations is given by eq.(A32). The  $x_n$  are then obtained by inserting  $y_m$  in eq.(A36). One gets

$$(A37) \quad x_m = \sum_{n=-\infty}^{+\infty} W_m^n g_n$$

with

$$(A38) \quad W_m^n = |n+\mu| |m+\mu| (-1)^{n+m-1} T_m^n(-u) + |m+\mu| \delta_m^n$$

Using the property of the Legendre function  $P_n(u)$ ,  $n$  integer

$$P_n(-u) = (-1)^n P_n(u) \frac{|n|}{n},$$

one gets the following representation of  $W_m^n$ :



$$(A39) \quad W_m^n = (n+\mu)V_m^n(u) + \mu P_m(u) \frac{1}{2} \left( P_{n-1}(u) + \frac{P_n(u)P_{\mu}(-u)}{P_{\mu-1}(-u)} \right).$$

The equations for  $y_n$  are solved assuming  $\mu \neq 0$ . But the limiting case  $\mu = 0$  is also included in the solution.